Linear spin waves in a trapped Bose gas

T. Nikuni*

Department of Physics, University of Toronto, Toronto, Ontario, Canada M5S 1A7

J. E. Williams and C. W. Clark

Electron and Optical Physics Division, National Institute of Standards and Technology, Gaithersburg, Maryland 20899-8410

An ultracold Bose gas of two-level atoms can be thought of as a spin-1/2 Bose gas. It supports spin-wave collective modes due to the exchange mean field. Such collective spin oscillations have been observed in recent experiments at JILA with ^{87}Rb atoms confined in a harmonic trap. We present a theory of the spin-wave collective modes based on the moment method for trapped gases. In the collisionless and hydrodynamic limits, we derive analytic expressions for the frequencies and damping rates of modes with dipole and quadrupole symmetry. We find that the frequency for a given mode is given by a temperature-independent function of the peak density n, and falls off as $1/n$. We also find that, to a very good approximation, excitations in the radial and axial directions are decoupled. We compare our model to the numerical integration of a one-dimensional version of the kinetic equation and find very good qualitative agreement. The damping rates, however, show the largest deviation for intermediate densities, where one expects Landau damping—which is unaccounted for in our moment approach—to play a significant role.

I. INTRODUCTION

Collective spin oscillations are a general consequence of the quantum exchange between identical particles in a system where a macroscopic symmetry breaking exists in spin space [1]. From a condensed matter perspective, spin waves are most familiar in strongly interacting degenerate Fermi systems, such as a ferromagnet. It is somewhat counter intuitive, although well established both experimentally [2–4] and theoretically [5–9], that collective spin behavior can also occur in nondegenerate dilute spin-polarized gases when the thermal de Broglie wavelength exceeds the effective range of interaction between two colliding atoms. In these systems, a transverse spin wave is excited by applying an inhomogeneous magnetic field followed by a small tipping pulse. It is remarkable that the mean field generates collective spin dynamics, but has no discernible effect on thermodynamic equilibrium properties since $gn/k_BT \ll 1$, where g is the binary interaction parameter, n is the density, and T the temperature.

Recent experiments at JILA [10,11] on a trapped ^{87}Rb gas have revived interest in spin waves in dilute gases [12–15]. These experiments offer several interesting new features compared to the earlier experiments in spin-polarized hydrogen [2,3], which take advantage of the technological advances made over the last twenty years in the measurement and control of cold atomic gases. A prominent feature of the new generation of experiments is the ability to take spatially resolved measurements of the gas sample using absorption imaging techniques. Another exciting advancement is the ability to cool the sample into the quantum degenerate re-

gime, which permits the study of spin waves in a Bose-Einstein-condensed gas at finite temperatures; this regime has never been investigated experimentally and has only received minor attention in the theoretical literature [16–18]. In this paper, however, we focus on the noncondensed regime relevant to the recent JILA experiments [10,11], where the temperatures are approximately twice that needed for Bose-Einstein condensation T_{BEC}.

The JILA system consists of a dilute gas of ^{87}Rb atoms that have been optically pumped into the $|F=1, M_F=-1\rangle$ $\equiv |1\rangle$ hyperfine state and are confined in a magnetic harmonic trapping potential. By applying microwave and radiofrequency radiation that couples to the $|2,1\rangle \equiv |2\rangle$ state, atoms in the gas can be uniformly prepared in an arbitrary superposition of the $|1\rangle$ and $|2\rangle$ states. This system can be thought of as a spin-1/2 system by taking $|1\rangle$ as the spin-up state and $|2\rangle$ as the spin-down state. In Fig. 1 we illustrate the corresponding Bloch vector spin describing the internal state of the atoms. Note that because the magnetic field direction varies in the trap [19], the spin axis shown in Fig. 1 is not isomorphic with the coordinate axis describing the position of an atom, in contrast to the situation in spin-polarized hydrogen.

In the JILA experiment, an initial $\pi/2$ pulse is applied to tip the spins into the transverse direction v. The spin vector then precesses about the longitudinal w axis at a rate proportional to the energy difference between hyperfine states. Due to the mean field and differential Zeeman effects, the local frequency splitting between hyperfine states varies approximately quadratically with position. This inhomogeneity initiates collective spin dynamics through the exchange mean field, the initial onset of which gives the striking appearance of spin segregation [10,12–14]. The inhomogeneous frequency splitting can be made arbitrarily small to study the linear response of the system. Recently this technique was used to probe intrinsic collective spin oscillations [11]. Stud-

————
*Present address: Department of Physics, Faculty of Science, Tokyo University of Science, 1-3 Kagurazaka, Shinjuku-ku, Tokyo 162-8601, Japan.
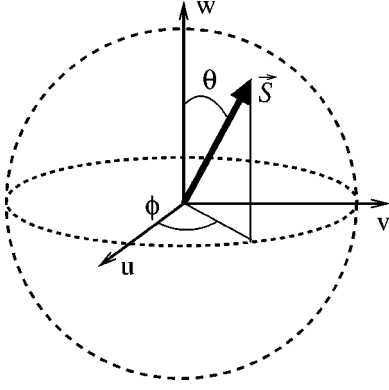
FIG. 1. Schematic diagram of the Bloch vector spin $\vec{S}$. The spins of the atoms are initially pointing up, $\vec{S}=\{0,0,S_w\}$, corresponding to all the atoms being in the state $|1\rangle$. After the $\pi/2$ pulse, the spin vector is pointing along the v axis, $\vec{S}=\{0,S_v,0\}$, corresponding to the state $(|1\rangle+i|2\rangle)/\sqrt{2}$.

ies of such spin-wave collective modes provide us clearer physical understanding of the important role of the exchange interactions in a dilute Bose gas.

The experiments described in Refs. [10,11] present spatially resolved images of spin dynamics in a gas. The density profile of either state is measured using absorption imaging. Together with the Ramsey fringe technique, integrated spatial profiles of the longitudinal spin S_w and transverse phase ϕ can be extracted from experimental data, as shown in the stunning images in Ref. [11]. This is in sharp contrast to the earlier hydrogen experiments, where a pulsed NMR technique is used to obtain the frequency of spin oscillation integrated over the entire sample. In this paper, we show a theoretical prediction of the spatial structure of the spin dynamics that qualitatively agrees with experimental observation.

In this paper, we present the theory of spin waves in a trapped Bose gas using the moment method [20,21], which was originally developed to study collective density oscillations in a trapped classical gas. The moment approach has also been applied to a rotating gas [22] and was recently generalized to treat a Bose-Einstein-condensed gas at finite temperature to study the scissors modes [23]. An advantage of this technique is that the solution maps smoothly between the collisionless and hydrodynamic regimes [20]. We apply the moment method to a spin kinetic equation, and derive explicit analytical expressions for frequency and damping of dipole and quadrupole modes in weak and strong coupling limits. We also numerically solve a one-dimensional (1D) model of the kinetic equation, and compare with the moment results.

II. SPIN KINETIC EQUATIONS

The Hamiltonian describing a single, trapped, two-level atoms of mass m is

$$\hat{H}=\left[-\frac{\hbar^2}{2m}\nabla^2+U_{\text{ext}}(\mathbf{r})\right]\hat{1}+\frac{\hbar}{2}\vec{\Omega}(\mathbf{r})\cdot\vec{\tau}. \qquad (1)$$

The first term in Eq. (1) is the center-of-mass Hamiltonian containing the kinetic energy and the external parabolic trap potential

$$U_{\text{ext}}(\mathbf{r})=\frac{m\omega_z^2}{2}[\alpha^2(x^2+y^2)+z^2], \qquad (2)$$

where $\alpha=\omega_\perp/\omega_z$. This part of the Hamiltonian is uncoupled from the internal, pseudospin, degree of freedom, which is governed by the second term: $\vec{\Omega}(\mathbf{r})\cdot\vec{\tau}=\Omega_u(\mathbf{r})\hat{\tau}_u+\Omega_v(\mathbf{r})\hat{\tau}_v+\Omega_w(\mathbf{r})\hat{\tau}_w$, where $\hat{\tau}_i$ is a Pauli matrix. In the absence of an external coupling field, $\Omega_u=\Omega_v=0$ and $\Omega_w=\Delta(\mathbf{r})$ [10,11] is the frequency splitting between the two states (we go to a rotating frame to eliminate the large hyperfine splitting ω_{hf} frequency). We model binary interactions between particles by a δ-function pseudopotential describing elastic, spin preserving collisions, the strength of which depends on the hyperfine states $V_{ij}(\mathbf{r},\mathbf{r}')=g_{ij}\delta(\mathbf{r}-\mathbf{r}')$, where $g_{ij}=4\pi\hbar^2 a_{ij}/m$, with a_{ij} being the scattering length for collisions between atoms of species i and j. For ^{87}Rb, $a_{11}=100.9a_0$, $a_{12}=98.2a_0$, $a_{22}=95.6a_0$, where a_0 is the Bohr radius [10]. In the rest of this paper, however, we make the simplification that $a_{11}=a_{22}=a_{12}\equiv a$, which is a reasonable approximation for ^{87}Rb.

Several groups have previously worked out the fundamental kinetic theory of a noncondensed dilute Bose gas with internal degrees of freedom, to describe spin waves in spin-polarized atomic hydrogen above T_{BEC} [6–9]. Using a semiclassical approximation to describe atomic motion in terms of a phase-space distribution function, we obtain coupled Boltzmann equations for the atomic $f(\mathbf{r},\mathbf{p},t)$ and spin $\vec{\sigma}(\mathbf{r},\mathbf{p},t)$ distribution functions:

$$\frac{\partial f}{\partial t}+\frac{\mathbf{p}}{m}\cdot\nabla_r f-\nabla U_n\cdot\nabla_p f-\frac{\hbar}{2}\nabla\Omega_{ni}\cdot\nabla_p\sigma_i=\left.\frac{\partial f}{\partial t}\right|_{\text{coll}}, \qquad (3)$$

$$\frac{\partial\vec{\sigma}}{\partial t}+\frac{\mathbf{p}}{m}\cdot\nabla_r\vec{\sigma}-\nabla U_n\cdot\nabla_p\vec{\sigma}-\frac{\hbar}{2}\nabla\vec{\Omega}_n\cdot\nabla_p f-\vec{\Omega}_n\times\vec{\sigma}$$

$$=\left.\frac{\partial\vec{\sigma}}{\partial t}\right|_{\text{coll}}. \qquad (4)$$

Equation (3) has an implicit sum over the repeated index $i=u,v,w$ in the fourth term. The total density and spin density are obtained from the distribution functions as $n(\mathbf{r},t)\equiv n_1(\mathbf{r},t)+n_2(\mathbf{r},t)=\int d\mathbf{p}f(\mathbf{r},\mathbf{p},t)/(2\pi\hbar)^3$ and $\vec{S}(\mathbf{r},t)=\int d\mathbf{p}\vec{\sigma}(\mathbf{r},\mathbf{p},t)/(2\pi\hbar)^3$, respectively. Here the longitudinal component of the spin represents the relative density $S_w=n_1-n_2$ and the transverse components S_u and S_v describe the real and imaginary parts of the internal coherence. The center-of-mass effective potential is $U_n(\mathbf{r},t)=U_{\text{ext}}(\mathbf{r})+3gn(\mathbf{r},t)/2$. The effective coupling field including mean-field effects is

$$\vec{\Omega}_n(\mathbf{r},t)=\vec{\Omega}(\mathbf{r},t)+\frac{g}{\hbar}\vec{S}(\mathbf{r},t). \qquad (5)$$

The collision integrals in Eqs. (3) and (4) are written explicitly in the Appendix.

The center of mass and spin are coupled via the third and fourth terms in both Eq. (3) and Eq. (4). These terms involve spatial gradients over the density and scale like $gn/k_BT \ll 1$, and thus can be neglected. This allows us to make the further simplification that the center of mass and spin dynamics are decoupled. Since we are interested in the intrinsic collective modes of the system, we also assume that the field $\vec{\Omega}(\mathbf{r}) = [0,0,\Delta(\mathbf{r})]$ can be made to vanish after the spin wave is excited. This assumption is motivated by the JILA experiment [11], where the static inhomogeneous frequency splitting could be adjusted to zero after a short excitation time. The position dependence of $\Delta(\mathbf{r})$ determines the symmetry of collective mode excited. With these two assumptions, the kinetic equation for the spin distribution function then simplifies to

$$\frac{\partial \vec{\sigma}}{\partial t} + \frac{\mathbf{p}}{m} \cdot \boldsymbol{\nabla} \vec{\sigma} - \boldsymbol{\nabla} U_{\text{ext}} \cdot \boldsymbol{\nabla}_p \vec{\sigma} - \frac{g}{\hbar} \vec{S} \times \vec{\sigma} = \frac{\partial \vec{\sigma}}{\partial t}\bigg|_{\text{coll}}. \quad (6)$$

In this paper, we consider small amplitude spin oscillations around a fully polarized state. It is convenient to define new spin coordinates (u',v',w') with w' being the direction of the initial spin polarization. In the experiment described in Ref. [11], the spin oscillations occur about the spin state polarized along the v axis. In this case one must make the mapping of the spin coordinates $(u',v',w') = (w,u,v)$, corresponding to a cyclic permutation [33]. We then linearize the kinetic equation around the equilibrium state polarized along the w' direction (we drop the prime from our notation from here on): $\sigma_{u0} = \sigma_{v0} = 0$, and $\sigma_{w0}(\mathbf{r},\mathbf{p}) = f_0(\mathbf{r},\mathbf{p})$, where the equilibrium distribution is

$$f_0(\mathbf{r},\mathbf{p}) = \exp\left\{-\beta\left[\frac{p^2}{2m} + U_{\text{ext}}(\mathbf{r}) - \mu_0\right]\right\}. \quad (7)$$

The equilibrium density given from Eq. (7) is

$$n_0(\mathbf{r}) = \int \frac{d\mathbf{p}}{(2\pi\hbar)^3} f_0(\mathbf{r},\mathbf{p}) = \frac{1}{\lambda_{\text{th}}^3} \exp[-\beta U_{\text{ext}}(\mathbf{r})], \quad (8)$$

where $\lambda_{\text{th}} = (2\pi\hbar^2/mk_BT)^{1/2}$ is the thermal de Broglie wavelength. We then substitute $\vec{\sigma}(\mathbf{r},\mathbf{p},t) = \vec{\sigma}_0(\mathbf{r},\mathbf{p}) + \delta\vec{\sigma}(\mathbf{r},\mathbf{p},t)$ into Eq. (6) to obtain the linearized spin kinetic equation

$$\frac{\partial \delta\vec{\sigma}}{\partial t} + \frac{\mathbf{p}}{m} \cdot \boldsymbol{\nabla} \delta\vec{\sigma} - \boldsymbol{\nabla} U_{\text{ext}} \cdot \boldsymbol{\nabla}_p \delta\vec{\sigma} - \frac{g}{\hbar}(\vec{S}_0 \times \delta\vec{\sigma} + \delta\vec{S} \times \vec{\sigma}_0)$$

$$= \frac{\partial \vec{\sigma}}{\partial t}\bigg|_{\text{coll}}. \quad (9)$$

The linearized form of the collision integral is discussed in the Appendix.

The longitudinal spin dynamics is described by

$$\frac{\partial \delta\sigma_w}{\partial t} + \frac{\mathbf{p}}{m} \cdot \boldsymbol{\nabla} \delta\sigma_w - \boldsymbol{\nabla} U_{\text{ext}} \cdot \boldsymbol{\nabla}_p \delta\sigma_w = \frac{\partial \delta\sigma_w}{\partial t}\bigg|_{\text{coll}}. \quad (10)$$

Since the mean-field term does not appear in Eq. (10), collective oscillations of the longitudinal spin only occur in the low-density collisionless regime in a trapped gas. In the high-density hydrodynamic regime, longitudinal modes become purely relaxational modes damped by the diffusion transport process. The crossover from the collisionless spin oscillation to the hydrodynamic relaxation mode in a longitudinal spin excitation was observed in a trapped ^{40}K Fermi gas [24,25] (although they were not excitations from the fully polarized state as considered here). In contrast, transverse spin waves behave collectively due to the mean field and will be the focus of this paper. For the transverse spin fluctuations, it is convenient to work with $\delta\sigma_{\pm} \equiv \delta\sigma_u \pm i\delta\sigma_v$. We then obtain

$$\frac{\partial \delta\sigma_{\pm}}{\partial t} + \frac{\mathbf{p}}{m} \cdot \boldsymbol{\nabla} \delta\sigma_{\pm} - \boldsymbol{\nabla} U_{\text{ext}} \cdot \boldsymbol{\nabla}_p \delta\sigma_{\pm}$$

$$\pm i\frac{g}{\hbar}(f_0\delta S_{\pm} - n_0\delta\sigma_{\pm}) = \frac{\partial \delta\sigma_{\pm}}{\partial t}\bigg|_{\text{coll}}. \quad (11)$$

Although we are interested in a trapped Bose gas, it is useful to summarize earlier results on the theory of spin waves in a homogeneous gas [26]. In the long wavelength limit, where the gas can be treated in the hydrodynamic regime, the dispersion relation has the form [8,26]

$$\omega(k) = -ik^2 v_{\text{th}}^2 \tilde{\tau}_D, \quad (12)$$

where $v_{\text{th}} = \sqrt{k_BT/m}$ and $\tilde{\tau}_D$ is a complex diffusive relaxation time. For transverse spin oscillations, one finds $\tilde{\tau}_D^{-1} = (\tau_D^{-1} - ign/\hbar)$, where the diffusive relaxation time is $\tau_D = [(32a^2n/3)\sqrt{\pi k_BT/m}]^{-1}$. Due to the exchange mean field, the transverse spin behaves collectively, and in the limit where $gn\tau_D/\hbar \gg 1$, the dispersion relation has the form

$$\omega(k) = \frac{\hbar k^2}{2m^*} - \frac{i}{\tau_D}\left(\frac{\hbar k v_{\text{th}}}{gn}\right)^2, \quad (13)$$

where $m^* = (gn/2k_BT)m$ is regarded as an effective mass. The k^2 dispersion relation is a universal result for ferromagneticlike spin systems [1]. The longitudinal spin oscillations do not behave collectively, but rather exhibit a purely diffusive mode, with $\tilde{\tau}_D \to \tau_D$ in Eq. (12).

III. MOMENT METHOD FOR A TRAPPED SPIN-1/2 GAS

We now turn to spin waves in a Bose gas confined in the harmonic trap potential. Starting from Eq. (11), one can derive a general set of coupled moment equations associated with a set of polynomial functions $\chi_i(\mathbf{r},\mathbf{p})$:

$$\frac{d\langle\chi_i\rangle}{dt} - \left\langle \boldsymbol{\nabla}\chi_i \cdot \frac{\mathbf{p}}{m}\right\rangle + \langle\boldsymbol{\nabla} U_{\text{ext}} \cdot \boldsymbol{\nabla}_p\chi_i\rangle$$

$$+ i\frac{g}{\hbar}[\langle S_+\chi_i\rangle_0 - \langle n_0\chi_i\rangle] = \langle\chi_i\rangle_{\text{coll}}, \quad (14)$$

where the moment variables are defined as

$$\langle \chi_i \rangle \equiv \frac{1}{N} \int d\mathbf{r} \int \frac{d\mathbf{p}}{(2\pi\hbar)^3} \chi_i(\mathbf{r},\mathbf{p}) \delta\sigma_+(\mathbf{r},\mathbf{p},t), \quad (15)$$

$$\langle \chi_i \rangle_{\text{coll}} \equiv \frac{1}{N} \int d\mathbf{r} \int \frac{d\mathbf{p}}{(2\pi\hbar)^3} \chi_i(\mathbf{r},\mathbf{p}) \frac{\partial \delta\sigma_+}{\partial t}\Big|_{\text{coll}}, \quad (16)$$

$$\langle \chi_i \rangle_0 \equiv \frac{1}{N} \int d\mathbf{r} \int \frac{d\mathbf{p}}{(2\pi\hbar)^3} \chi_i(\mathbf{r},\mathbf{p}) f_0(\mathbf{r},\mathbf{p}). \quad (17)$$

In general, moment equations are not closed since the mean field and collisional terms couple to higher moments. Those higher moments can be truncated by expanding the fluctuations in the distribution function $\delta\sigma_+$ in powers of position and momentum. One can relate the coefficients in the expansion to the moments of the distribution function $\langle \chi_i \rangle$ to yield a closed set of equations that can be solved analytically.

The choice of the functions χ_i depends on the symmetry of the spin-wave mode we are interested in. In the following sections, we consider the dipole and quadrupole oscillations.

A. Dipole mode

We first consider the spin-wave collective mode with a dipole symmetry, which could be excited by a linear inhomogeneous frequency splitting, such as $\Delta(\mathbf{r}) \propto z$. For our set of moments to describe this oscillation, we choose

$$\chi_1 = x_i, \ \chi_2 = p_{x_i}/m. \quad (18)$$

The subscript indicates the axis along which the excitation oscillates $x_i \in \{x,y,z\}$. Within the moment method approximate treatment, the dipole modes along the three axes are completely decoupled. We also define $\chi_0 = 1$, related to the norm of $\delta\sigma_+$; we set $\langle \chi_0 \rangle = 0$, which is required from the conservation of the spin density.

From Eq. (14), the equations of motion for the moments Eq. (18) are given by

$$\frac{d}{dt}\langle \chi_1 \rangle = \langle \chi_2 \rangle, \quad (19)$$

$$\frac{d}{dt}\langle \chi_2 \rangle + \omega_i^2 \langle \chi_1 \rangle - i\frac{g}{\hbar}\langle n_0 \chi_2 \rangle = \langle \chi_2 \rangle_{\text{coll}}, \quad (20)$$

where ω_i is either ω_z for an axial mode or $\omega_\perp$ for a radial mode. These are not a closed set of equations, since in general the mean field and collisional terms in Eq. (20) couple to higher moments. The hierarchy of moment equations can be truncated by assuming the explicit truncated form for the distribution $\delta\sigma_+$:

$$\delta\sigma_+ = f_0[\alpha_0 + \alpha_1 x_i + \alpha_2 p_{x_i}]. \quad (21)$$

The coefficients in the expansion can be related back to the set of moments using Eq. (15): $\alpha_0 = 0$, $\alpha_1 = (m\omega_i^2/k_BT)\langle \chi_1 \rangle$, and $\alpha_2 = \langle \chi_2 \rangle/k_BT$.

Using the explicit form for $\delta\sigma_+$ in Eq. (21), the mean-field and collisional terms can be expressed in terms of the dipole moments. The resulting closed set of coupled moment equations, written in matrix form, is

$$\frac{d}{dt}\chi = \hat{W}_d \chi, \quad (22)$$

where the coupling matrix $\hat{W}_d$ is

$$\hat{W}_d = -\begin{pmatrix} 0 & -1 \\ \omega_i^2 & (\gamma_D - i\omega_{\text{MF}}) \end{pmatrix}. \quad (23)$$

Here we have defined the vector of moments $\chi \equiv \{\langle \chi_1 \rangle, \langle \chi_2 \rangle\}$. Three different frequencies appear in $\hat{W}_d$: the trap frequency ω_i along the axis of oscillation, the mean-field frequency ω_{MF} defined by the spatial average $\omega_{\text{MF}} \equiv \int d\mathbf{r} g n_0^2(\mathbf{r})/N\hbar$,

$$\omega_{\text{MF}} = \frac{g n_0(0)}{2\sqrt{2}\hbar}, \quad (24)$$

and the spatially averaged diffusion relaxation rate γ_D, the form of which is given in the discussion in the Appendix.

We now look for normal mode solutions $\chi = \chi_0 e^{-i\omega t}$. Substituting this into Eq. (22) yields an eigenvalue equation with two solutions. It is straightforward to show that the mode frequencies ω obey the dispersion relation

$$\omega^2 + i\tilde{\gamma}_D \omega - \omega_i^2 = 0, \quad (25)$$

where $\tilde{\gamma}_D \equiv \gamma_D - i\omega_{\text{MF}}$ is the effective (complex) diffusion relaxation rate including the mean-field effect. The solution is given by

$$\omega = \frac{1}{2}[-i\tilde{\gamma}_D \pm \sqrt{4\omega_i^2 - \tilde{\gamma}_D^2}]. \quad (26)$$

We shall consider two limiting cases to obtain the scaling behavior of the frequency and damping of the modes. In the weak interaction, or collisionless, limit where $\omega_i \gg |\tilde{\gamma}_D|$, one has

$$\omega \simeq \pm \omega_i - \frac{\omega_{\text{MF}}}{2} - i\frac{\gamma_D}{2}. \quad (27)$$

In the strong coupling, or hydrodynamic, limit where $\omega_i \ll |\tilde{\gamma}_D|$, one has

$$\omega \simeq \begin{cases} -i\omega_i^2/\tilde{\gamma}_D & \text{(low)} \\ -i\tilde{\gamma}_D & \text{(high)}. \end{cases} \quad (28)$$

These represent low- and high-frequency modes, with the low-frequency mode having a higher $Q \sim \text{Re}\omega/\text{Im}\omega$ value. The low-frequency solution has the form of the diffusion relaxation rate with a complex diffusion coefficient. More explicitly, the dispersion relation in the strong-coupling limit takes the approximate form

$$\omega \simeq \frac{\omega_i^2}{\omega_{MF}}\left(1-\frac{\gamma_D^2}{\omega_{MF}^2}-i\frac{\gamma_D}{\omega_{MF}}\right). \qquad (29)$$

The scaling behavior of the real part of Eq. (29) can be recovered in a simple model based on the homogeneous gas result of Eq. (12). For low-frequency collective modes in a trapped gas along the x_i direction, the wave vector k is estimated as $k \sim 1/R_i$, where $R_i = m\omega_i/k_B T$ is the size of the cloud along the x_i direction.

B. Quadrupole mode

In the JILA experiment [11], a spin-wave collective mode with a quadrupole symmetry is excited due to an approximately quadratically varying frequency splitting $\Delta(\mathbf{r}) \propto z^2$. In principle, the oscillation may be excited along both the axial or radial directions, and so we take the following quantities for our set of moments:

$$\chi_1 = z^2, \quad \chi_2 = zp_z/m, \quad \chi_3 = p_z^2/m^2, \qquad (30)$$

$$\chi_4 = r_\perp^2, \quad \chi_5 = \mathbf{r}_\perp \cdot \mathbf{p}_\perp/m, \quad \chi_6 = p_\perp^2/m^2, \qquad (31)$$

where $r_\perp = \sqrt{x^2+y^2}$ and $p_\perp = \sqrt{p_x^2+p_y^2}$. We also define $\chi_0 = 1$, related to the norm of $\delta\sigma$, which we set to zero $\langle\chi_0\rangle = 0$.

The six moment equations for the above quantities are

$$\frac{d\langle\chi_1\rangle}{dt} - 2\langle\chi_2\rangle = 0, \qquad (32)$$

$$\frac{d\langle\chi_2\rangle}{dt} - \langle\chi_3\rangle + \omega_z^2\langle\chi_1\rangle - i\frac{g}{\hbar}\langle n_0\chi_2\rangle = \langle\chi_2\rangle_{coll}, \qquad (33)$$

$$\frac{d\langle\chi_3\rangle}{dt} + 2\omega_z^2\langle\chi_2\rangle + i\frac{g}{\hbar}[\langle S_+\chi_3\rangle_0 - \langle n_0\chi_3\rangle] = \langle\chi_3\rangle_{coll}, \qquad (34)$$

$$\frac{d\langle\chi_4\rangle}{dt} - 2\langle\chi_5\rangle = 0, \qquad (35)$$

$$\frac{d\langle\chi_5\rangle}{dt} - \langle\chi_6\rangle + \omega_\perp^2\langle\chi_4\rangle - i\frac{g}{\hbar}\langle n_0\chi_5\rangle = \langle\chi_5\rangle_{coll}, \qquad (36)$$

$$\frac{d\langle\chi_6\rangle}{dt} + 2\omega_\perp^2\langle\chi_5\rangle + i\frac{g}{\hbar}[\langle S_+\chi_6\rangle_0 - \langle n_0\chi_6\rangle] = \langle\chi_6\rangle_{coll}. \qquad (37)$$

Just as in the previous case of the dipole mode, we truncate the hierarchy by assuming an appropriate form for the distribution

$$\delta\sigma_+ = f_0[\alpha_0 + \alpha_1 z^2 + \alpha_2 zp_z + \alpha_3 p_z^2 \\ + \alpha_4 r_\perp^2 + \alpha_5 \mathbf{r}_\perp \cdot \mathbf{p}_\perp + \alpha_6 p_\perp^2]. \qquad (38)$$

The coefficients in the expansion can be related back to the set of moments using Eq. (15): $\alpha_0 = -m[\omega_z^2\langle\chi_1\rangle + \omega_\perp^2\langle\chi_4\rangle + \langle\chi_3\rangle + \langle\chi_6\rangle]/2k_B T$, $\alpha_1 = (m\omega_z^2/k_B T)^2\langle\chi_1\rangle/2$, $\alpha_2 = m\omega_z^2\langle\chi_2\rangle/$

$(k_B T)^2$, $\alpha_3 = \langle\chi_3\rangle/2(k_B T)^2$, $\alpha_4 = (m\omega_\perp^2/k_B T)^2\langle\chi_4\rangle/2$, $\alpha_5 = m\omega_\perp^2\langle\chi_5\rangle/(k_B T)^2$, and $\alpha_6 = \langle\chi_6\rangle/2(k_B T)^2$.

Following the same procedure as for the dipole mode, we obtain a closed set of coupled moment equations, written in matrix form as

$$\frac{d}{dt}\chi = \hat{W}_q\chi, \qquad (39)$$

where the coupling matrix $\hat{W}_q$ in this case is

$$\hat{W}_q = -\begin{pmatrix} 0 & -2 & 0 & 0 & 0 & 0 \\ \omega_z^2 & \tilde{\gamma}_D/2 & -1 & 0 & 0 & 0 \\ 0 & 2\omega_z^2 & \tilde{\gamma}_T^z & 0 & 0 & \delta\gamma_T \\ 0 & 0 & 0 & 0 & -2 & 0 \\ 0 & 0 & 0 & \omega_\perp^2 & \tilde{\gamma}_D/2 & -1 \\ 0 & 0 & 2\delta\gamma_T & 0 & 2\omega_\perp^2 & \tilde{\gamma}_T^\perp \end{pmatrix}. \qquad (40)$$

The vector of moments is $\chi \equiv \{\langle\chi_1\rangle, \langle\chi_2\rangle, \ldots, \langle\chi_6\rangle\}$. The tilde on the relaxation rates indicates the complex form $\tilde{\gamma} = (\gamma - i\omega_{MF})$. The quantities γ_T^z and $\gamma_T^\perp$, given explicitly in the Appendix, are the spatially averaged axial and radial thermal relaxation rates, the difference of which $\delta\gamma = \gamma_T^\perp - \gamma_T^z$ is not zero in general. We note that $\hat{W}_q$ is nearly block diagonal and that the axial and radial oscillations are coupled only through collisions associated with $\delta\gamma_T$.

By substituting $\chi = \chi_0 e^{-i\omega t}$ into Eq. (39), we obtain an eigenvalue equation with six solutions; the dispersion law is determined from

$$\mathcal{F}_1^z(\omega)\mathcal{F}_1^\perp(\omega) + \mathcal{F}_2(\omega)\mathcal{F}_3(\omega) = 0, \qquad (41)$$

where

$$\mathcal{F}_1^i(\omega) = \left(\omega^2 - 4\omega_i^2 + \frac{2\omega_i^2}{1-i\omega/\tilde{\gamma}_T^i} + i\omega\frac{\tilde{\gamma}_D}{2}\right), \qquad (42)$$

$$F_2(\omega) = (\omega + i\tilde{\gamma}_T^z)(\omega + i\tilde{\gamma}_T^\perp), \qquad (43)$$

$$\mathcal{F}_3(\omega) = 2\delta\gamma_T^2\left(\omega^2 - 2\omega_z^2 + i\omega\frac{\tilde{\gamma}_D}{2}\right)\left(\omega^2 - 2\omega_\perp^2 + i\omega\frac{\tilde{\gamma}_D}{2}\right). \qquad (44)$$

In both the weak interaction ($\omega_i \gg |\tilde{\gamma}_D|, |\tilde{\gamma}_T^i|$) and strong interaction ($\omega_i \ll |\tilde{\gamma}_D|, |\tilde{\gamma}_T^i|$) limits, the axial and radial modes are uncoupled and are determined from $\mathcal{F}_1^i(\omega) = 0$, with $\mathcal{F}_1^i(\omega)$ given in Eq. (42). In the weak interaction limit, one has three modes,

$$\omega = 2\omega_i - \frac{\omega_{MF}}{2} - \frac{i}{4}(\gamma_D + \gamma_T^i), \qquad (45)$$

$$\omega = -\left(2\omega_i + \frac{\omega_{MF}}{2}\right) - \frac{i}{4}(\gamma_D + \gamma_T^i), \quad (46)$$

$$\omega = -\frac{\omega_{MF}}{2} - \frac{i}{2}\gamma_T^i. \quad (47)$$

In the strong interaction limit, there is one (weakly damped) low-frequency mode and two (strongly damped) high-frequency modes. The low-frequency mode is given by $\omega = -4i\omega_i^2/\widetilde{\gamma}_D$, which can be written approximately as

$$\omega \simeq \frac{4\omega_i^2}{\omega_{MF}}\left(1 - \frac{\gamma_D^2}{\omega_{MF}^2} - i\frac{\gamma_D}{\omega_{MF}}\right). \quad (48)$$

This has the same scaling behavior with respect to the density, scattering length, and temperature as the dipole mode result in Eq. (29).

IV. NUMERICAL SOLUTION OF THE 1D SPIN KINETIC EQUATION

In this section we compare the predictions of the moment method to a direct numerical solution of the spin kinetic equation. In Refs. [13,14], a one-dimensional model of the kinetic equation was presented and found to give very good agreement with experiments [10]. A justification that was given for the model is the separation of time scales between the axial and radial directions. In hindsight, the success of the one-dimensional model can be further understood based on the moment method results in the previous section that the axial and radial modes are uncoupled in the linearized regime.

We construct a one-dimensional model of the system by making the ansatz $\vec{\sigma}(\mathbf{r},\mathbf{p},t) = \vec{\sigma}(z,p,t)h_0(\mathbf{r}_\perp,\mathbf{p}_\perp)$ and then averaging over $\mathbf{r}_\perp$ and $\mathbf{p}_\perp$. Here we take the static profile in the radial direction to be of Gaussian form $h_0 = \exp[-(p_\perp^2/2m + m\omega_\perp^2 r_\perp^2/2)/k_B T]$. We substitute this ansatz into Eq. (4) and integrate over the radial phase-space variables, which gives the following one-dimensional model Boltzmann equation:

$$\frac{\partial\vec{\sigma}}{\partial t} + \frac{p}{m}\frac{\partial\vec{\sigma}}{\partial z} - \frac{\partial U_{ext}}{\partial z}\frac{\partial\vec{\sigma}}{\partial p} - \vec{\Omega}_n \times \vec{\sigma} = \frac{\partial\vec{\sigma}}{\partial t}\bigg|_{1D}. \quad (49)$$

Here we have dropped terms that scale like $gn/k_B T$. The collision integral in one-dimension involves a phase-space average in the radial direction $\partial\vec{\sigma}/\partial t|_{1D} \equiv \int_{xy}\partial\vec{\sigma}/\partial t|_{coll}/\int_{xy}h_0$, where we have introduced the notation $\int_{xy}\cdots \equiv \int d\mathbf{r}_\perp \int d\mathbf{p}_\perp \cdots/(2\pi\hbar)^2$. The radial averaging introduces a scaling factor in the mean-field terms, so that $g \to g' = g/(2\lambda_{th}^2)$, where λ_{th} is the thermal de Broglie wavelength. g' has the correct units of energy times distance required in our one-dimensional model.

Although the direct numerical simulation using the full expression for the one-dimensional collision integral derived from Eq. (A2) is technically feasible, we introduce a simple model for the relaxation
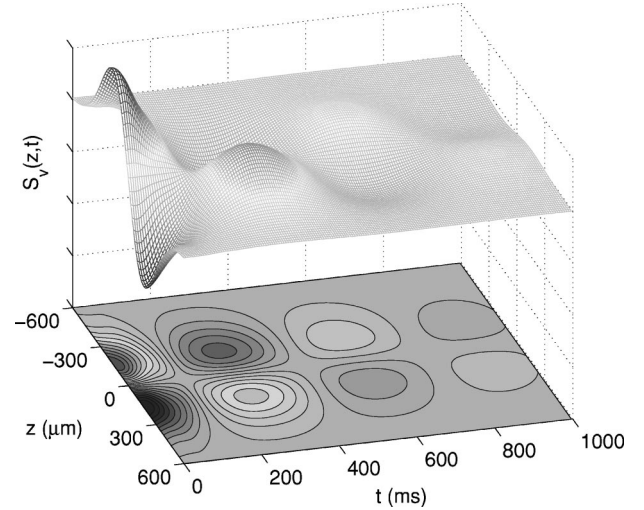

FIG. 2. Dipole excitation. The surface shows how the spin component $S_v(z,t)$ varies with position and time. For visual clarity, we also show the contours projected below the surface.

$$\frac{\partial\vec{\sigma}}{\partial t}\bigg|_{1D} = -\frac{1}{\tau_{cl}(z)}[\vec{\sigma}(z,p,t) - \vec{M}(z,t)f_0(z,p)], \quad (50)$$

where $\tau_{cl}(z) = [16a_{12}^2 n_0(z)\sqrt{\pi k_B T/m}]^{-1}$ is the radially averaged mean-collision time, $f_0(z,p) \equiv f_0(\mathbf{r},\mathbf{p})/h_0$, and $\vec{M}(z,t) = \vec{S}(z,t)/n_0(z)$. Equation (50) contains the essential properties of collisions: (i) it vanishes when the distribution function has the local equilibrium form $\vec{\sigma}(z,p,t) \propto \vec{M}(z,t)e^{-p^2/2mk_B T}$, (ii) it conserves the spin density. We note that the form Eq. (50) does not require the knowledge of the long-time equilibrium solution for $\vec{S}(\mathbf{r},t)$.

We solve Eq. (49) numerically using a finite difference, alternating-direction Crank-Nicholson routine. As a check on the numerics we monitor the integrated spin components $\int dz S_i(z,t)$, which are conserved if $\vec{\Omega} = 0$, and the integrated spin magnitude, which must satisfy the relation

$$\frac{\partial}{\partial t}\int dz(S_x^2 + S_y^2 + S_z^2) = 2\int dz\vec{J}\cdot\frac{d\vec{S}}{dz}. \quad (51)$$

The total spin can decay to zero if there is an inhomogeneous field $\vec{\Omega}(z,t)$ present (i.e., $\nabla\vec{\Omega} \neq 0$).

To compare directly with the moment method results derived in the previous section, we take as an initial state $\vec{\sigma}(z,t=0) = \vec{\sigma}_0(z) + \delta\vec{\sigma}(z)$, where $\vec{\sigma}_0(z) = \{0,0,f_0(z)\}$ and $\delta\vec{\sigma}(z) = \{\text{Re}\,\delta\sigma_+(z), \text{Im}\,\delta\sigma_+(z), 0\}$. We take $\delta\sigma_+$ of the form given in Eq. (21) for the dipole mode and Eq. (38), for the quadrupole mode. The coefficients α_i are determined by diagonalizing the coupling matrices Eq. (23) and Eq. (40), respectively (in this section we consider only the low-frequency excitations for a given symmetry).

In order to visualize the spatial form of the spin wave, we show the transverse spin component $S_v(z,t)$ in Figs. 2 and 3 as a function of position and time to show the symmetry of the dipole and quadrupole modes. We note the qualitative
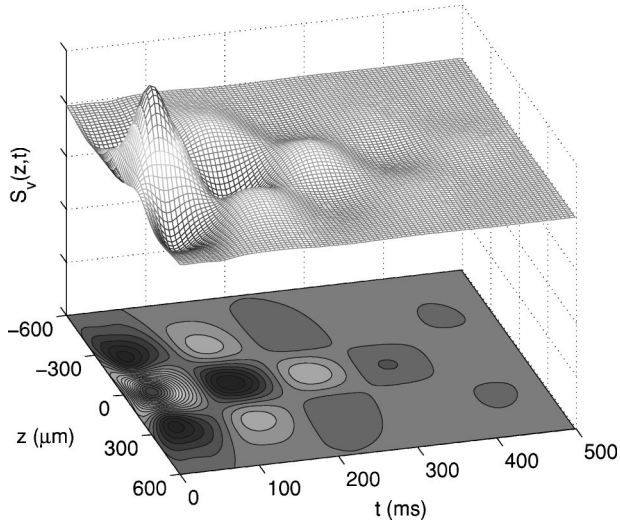
FIG. 3. Quadrupole excitation, as in Fig. 2.

FIG. 4. Frequency and damping rate of the dipole mode versus peak total density $n_0(0)$. The solid line is the low-frequency solution obtained from Eq. (25) and the chain and dashed lines are the weak Eq. (27) and strong Eq. (29) interaction limits, respectively. The points are obtained from a direct numerical solution of Eq. (49) for three different temperatures T: 600 nK (circle), 800 nK (diamond), and 1 mK (square).

agreement between the contours of Fig. 3 and the graph shown in Fig. 1(b) of Ref. [11]. We do not plot the $S_u(z,t)$ component, which has the same structure but is shifted 90° out-of-phase in time. The transverse spin $\{S_u(z,t), S_v(z,t)\}$ at a given position z traces out a spiral that terminates at the origin as $t \to \infty$, whose overall diameter varies with position. The spin precession as a function of position for the actual experiment is shown in Fig. 2 of Ref. [11].

We extract a frequency and damping rate from the numerical solution by calculating the dipole $\langle z \rangle$ or quadrupole $\langle z^2 \rangle$ moment and fitting this quantity to a damped sine function of the form $A \exp(-Bt)\sin(Ct+D)$. The coefficients are obtained using a least squares fitting routine. The frequency $\omega = C$ and damping rate $\gamma = B$ are then compared to the predictions of the moment method.

In Figs. 4 and 5 we plot the frequencies and damping rates for the dipole and quadrupole spin waves. We take values for the physical quantities corresponding to the JILA experiment, where $\omega_z/2\pi = 7$ Hz, and $\omega_\perp/2\pi = 230$ Hz. We find that the frequencies obtained from the numerical solution agree extremely well with the moment method prediction for the dipole mode, while the quadrupole mode shows only qualitative agreement. We also find that the frequencies in Figs. 4 and 5 are given as temperature-independent functions of the peak density, which is consistent with the moment results. In general, one can show that the streaming term of the linearized spin kinetic equation in Eq. (11) is invariant under the scale transformation $T \to T', \mathbf{r} \to (T'/T)^{1/2}\mathbf{r}, \mathbf{p} \to (T'/T)^{1/2}\mathbf{p}$ for given $n_0(0)$, and thus the frequency of any given mode is temperature independent. In Figs. 4 and 5 we do not show the damping as a function of temperature, which scales approximately as $\sqrt{T}$ at fixed peak density, according to Eq. (A20).

The most interesting feature occurs in the damping, where we see that the damping of the quadrupole mode is qualitatively different from that predicted by the moment method. We postulate that this difference, which is largest at intermediate densities, is due to Landau-type damping arising from the mean-field coupling of the collective mode to higher ex-
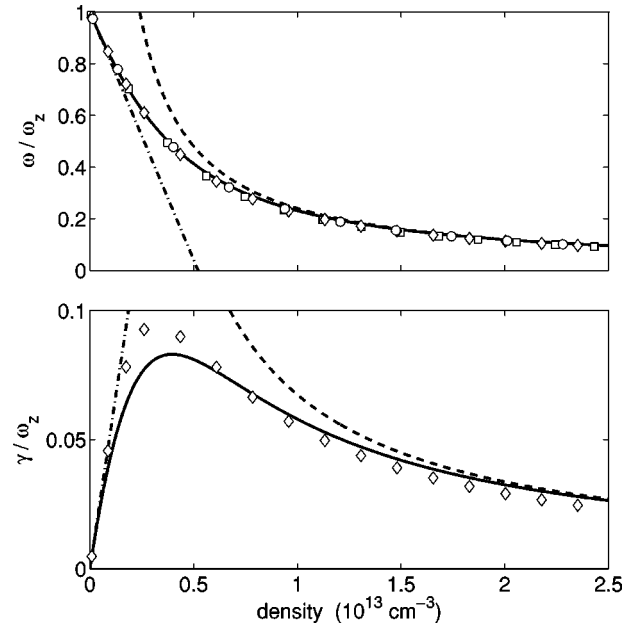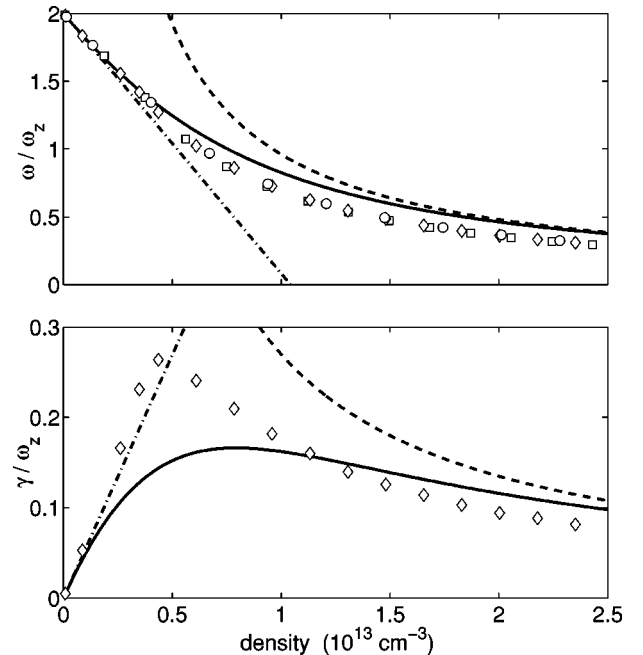

FIG. 5. Frequency and damping rate of the quadrupole mode versus peak total density $n_0(0)$. The solid line is the low-frequency solution obtained from Eq. (42) (e.g., $\mathcal{F}_1^z = 0$) and the chain and dashed lines are the weak Eq. (45) and strong Eq. (48) interaction limits, respectively. The points are obtained from a direct numerical solution of Eq. (49) for three different temperatures T: 600 nK (circle), 800 nK (diamond), and 1 mK (square).

citations. Our moment approach using the simple truncated form for the distribution function σ_+, as given by Eqs. (21) or (38), does not account for this effect [23].

For a homogeneous Bose gas, Oktel, and Levitov worked out the spectrum of spin waves in the collisionless regime [16] using a linear-response theory with the random-phase approximation. They find that the mean-field coupling gives rise to Landau-type damping, which is in addition to the collisional damping due to spin diffusion. The damping rate is given by

$$\gamma_L = \frac{\sqrt{\pi} g^2 n^2}{\hbar^2 k v_{\text{th}}} e^{-(gn/\hbar k v_{\text{th}})^2}. \tag{52}$$

A rough estimate of Landau damping in a trapped gas may be given by using $k \sim 1/R_{\text{th}}$ in this uniform gas result. However, this simple estimate predicts a damping rate that is about an order of magnitude larger than that shown in Fig. 5. Apparently one needs to work out the linear response calculation taking into account the excitation spectrum explicitly in a trap potential in order to obtain a better quantitative model for Landau damping.

In Ref. [11], we compare the numerical solution presented in this paper to experimental data, and find excellent agreement for both frequency and damping. It is important to realize that in our numerical calculation, we have used a relaxation time approximation to treat the collision integral. In this model, one has some freedom to choose an appropriate relaxation time; there are a few different candidates, but here we have used the spatially dependent form of the mean-collision time given in Eq. (50). Although this is a reasonable choice, it was not *a priori* obvious that it would result in the best agreement with experimental data.

We also remark that our results are strictly valid for the case where the inhomogeneity $\Delta(\mathbf{r})$ is vanishingly small (though we have not carried out the full linear response theory, we envision $\Delta(\mathbf{r})$ as playing the role of an external perturbation used to excite the spin wave). In the JILA experiment [11], the effect of applying a constant static $\Delta(\mathbf{r})$ during the entire spin-wave oscillation was investigated as a function of the magnitude of the perturbation. For a large inhomogeneity, the response of the system is nonlinear and the mode frequency is modified; the earlier JILA experiment [10] seems to reside in this regime.

V. CONCLUSION

In this paper, we have studied spin waves in a dilute non-condensed Bose gas of two-level atoms. Our main contribution is that we have treated an inhomogeneous system held in a harmonic trap in order to describe related experiments on spin waves [11]. We applied the moment method technique for dilute trapped gases, which lead to closed form solutions for the frequencies and damping of dipole and quadrupole modes. As a test of the validity of our moment model, we compared the results to the numerical calculation of a one-dimensional model of the spin Boltzmann equation and found very good agreement overall. The main discrepancy between the moment model and the numerical calculation

occurred in the damping of the quadrupole mode. We attribute this to the Landau damping, which is contained in the numerical approach, but absent in the moment model.

Although the salient features of spin waves in a noncondensed dilute gas seem to be well described by our theory, which shows excellent agreement with experimental data presented in Ref. [11], the situation for this system just below the Bose-Einstein-condensation temperature [18] remains largely unexplored. Many *zero temperature* properties of a spin-1/2 condensate have been studied, when the thermal component is absent, such as spin winding [27] and vortexlike spin textures [28,29]. It should be noted, however, that at zero temperature the condensate does not support spin waves of the type considered in this paper, since the exchange mechanism does not occur in the condensate. It is very interesting that the spin-1/2 thermal gas exhibits strong collective behavior in the spin dynamics due to the exchange effect, even in the collisionless regime; this is in sharp contrast to the behavior of density fluctuations of a single component thermal gas, where the mean field of the noncondensate plays a very minor role (mainly as a source of damping of the condensate excitations) [30,31]. At finite temperatures, the spins of the condensate and thermal gas will interact strongly. For future studies, it will be interesting to investigate how long-lived spin textures in the condensate are affected by the thermal gas, which in principle can itself support (probably short-lived) spin textures. It will also be important to understand how the condensate modifies spin waves in the thermal cloud [17].

APPENDIX: COLLISION INTEGRALS AND RELAXATION TIMES

The collision integrals appearing in the kinetic equations Eqs. (3) and (4) for the center of mass and spin distribution functions are given by

$$\frac{\partial f}{\partial t}\bigg|_{\text{coll}} = \frac{\pi g^2}{\hbar} \int \frac{d\mathbf{p}_2}{(2\pi\hbar)^3} \int \frac{d\mathbf{p}_3}{(2\pi\hbar)^3} \int d\mathbf{p}_4 \delta(\epsilon_p + \epsilon_{p_2}$$
$$+ \epsilon_{p_3} + \epsilon_{p_4}) \delta(\mathbf{p} + \mathbf{p}_2 - \mathbf{p}_3 - \mathbf{p}_4)\{3[f(\mathbf{p}_3)f(\mathbf{p}_4)$$
$$- f(\mathbf{p})f(\mathbf{p}_2)] + \vec{\sigma}(\mathbf{p}_3)\cdot\vec{\sigma}(\mathbf{p}_4) - \vec{\sigma}(\mathbf{p})\cdot\vec{\sigma}(\mathbf{p}_2)\}, \tag{A1}$$

$$\frac{\partial \vec{\sigma}}{\partial t}\bigg|_{\text{coll}} = \frac{\pi g^2}{\hbar} \int \frac{d\mathbf{p}_2}{(2\pi\hbar)^3} \int \frac{d\mathbf{p}_3}{(2\pi\hbar)^3} \int d\mathbf{p}_4 \delta(\epsilon_p + \epsilon_{p_2}$$
$$- \epsilon_{p_3} - \epsilon_{p_4}) \delta(\mathbf{p} + \mathbf{p}_2 - \mathbf{p}_3 - \mathbf{p}_4)\{3f(\mathbf{p}_3)\vec{\sigma}(\mathbf{p}_4)$$
$$+ \vec{\sigma}(\mathbf{p}_3)f(\mathbf{p}_4) - f(\mathbf{p})\vec{\sigma}(\mathbf{p}_2) - 3\vec{\sigma}(\mathbf{p})f(\mathbf{p}_2)\}, \tag{A2}$$

where $\epsilon_p \equiv p^2/2m$. Here we neglect a principal value contribution, which gives a second-order correction to the free streaming evolution, and we take all scattering lengths a_{ij} to be equal—a reasonable approximation for ^{87}Rb. This approximation results in the conservation of spin density during collisions, i.e., $\int d\mathbf{p} \, \partial\vec{\sigma}/\partial t|_{\text{coll}} = 0$. When the small differences in scattering lengths are accounted for, the transverse spin decays slowly. For ^{87}Rb, this contribution to the "$T2$" lifetime is of the order of 10 s [18].

For the linearized form of the spin collision term appearing in Eq. (9), it is convenient to express the fluctuation of the spin distribution function as

$$\delta\vec{\sigma}(\mathbf{r},\mathbf{p},t) = f_0(\mathbf{r},\mathbf{p})\vec{\psi}(\mathbf{r},\mathbf{p},t). \tag{A3}$$

Then the linearized collision integral is written as $\partial\vec{\sigma}/\partial t|_{\text{coll}} \equiv L[\vec{\psi}]$,

$$L[\vec{\psi}] = \frac{\pi g^2}{\hbar} \int \frac{d\mathbf{p}_2}{(2\pi\hbar)^3} \int \frac{d\mathbf{p}_3}{(2\pi\hbar)^3} \int d\mathbf{p}_4$$

$$\times \delta(\epsilon_p + \epsilon_{p_2} - \epsilon_{p_3} - \epsilon_{p_4}) \delta(\mathbf{p} + \mathbf{p}_2 - \mathbf{p}_3 - \mathbf{p}_4)$$

$$\times f_0(\mathbf{p}_3) f_0(\mathbf{p}_4) \{2[\vec{\psi}(\mathbf{p}_4) - \vec{\psi}(\mathbf{p})]$$

$$+ [\vec{\psi}(\mathbf{p}_4) + \vec{\psi}(\mathbf{p}_3) - \vec{\psi}(\mathbf{p}_2) + \vec{\psi}(\mathbf{p})]\}. \tag{A4}$$

Using the approximate forms of the distribution function Eqs. (21) and (38) in the linear collision operator and taking moments, we find that the collisional contributions to the moment equations are given by

$$\langle p_{x_i} \rangle_{\text{coll}} = -\gamma_D \langle p_{x_i} \rangle, \tag{A5}$$

$$\langle z p_z \rangle_{\text{coll}} = -\frac{\gamma_D}{2} \langle z p_z \rangle, \tag{A6}$$

$$\langle \mathbf{r}_\perp \cdot \mathbf{p}_\perp \rangle_{\text{coll}} = -\frac{\gamma_D}{2} \langle \mathbf{r}_\perp \cdot \mathbf{p}_\perp \rangle, \tag{A7}$$

$$\langle p_z^2 \rangle_{\text{coll}} = -\gamma_T^z \langle p_z^2 \rangle - \delta\gamma_T \langle p_\perp^2 \rangle, \tag{A8}$$

$$\langle p_\perp^2 \rangle_{\text{coll}} = -\gamma_T' \langle p_\perp^2 \rangle - 2\delta\gamma_T \langle p_z^2 \rangle. \tag{A9}$$

The various relaxation rates are given by spatial average of the following spin transport relaxation times:

$$\frac{n_0(\mathbf{r})}{\tau_D(\mathbf{r})} \equiv -\frac{1}{3mk_BT} \int \frac{d\mathbf{p}}{(2\pi\hbar)^3} \mathbf{p} L[\mathbf{p}], \tag{A10}$$

$$\frac{n_0(\mathbf{r})}{\tau_T(\mathbf{r})} \equiv -\int \frac{d\mathbf{p}}{(2\pi\hbar)^3} \frac{1}{2(mk_BT)^2} p_z^2 L[p_z^2], \tag{A11}$$

$$\frac{n_0(\mathbf{r})}{\tau_T^\perp(\mathbf{r})} \equiv -\int \frac{d\mathbf{p}}{(2\pi\hbar)^3} \frac{1}{4(mk_BT)^2} p_\perp^2 L[p_\perp^2]. \tag{A12}$$

The associated spatially averaged relaxation rates are given by

$$\gamma_D \equiv \frac{1}{N} \int d\mathbf{r} \frac{n_0(\mathbf{r})}{\tau_D(\mathbf{r})} = \frac{1}{2\sqrt{2}} \frac{1}{\tau_D(0)}, \tag{A13}$$

$$\gamma_T^z \equiv \frac{1}{N} \int d\mathbf{r} \frac{n_0(\mathbf{r})}{\tau_T(\mathbf{r})} = \frac{1}{2\sqrt{2}\,\tau_T^z(0)}, \tag{A14}$$

$$\gamma_T^\perp \equiv \frac{1}{N} \int d\mathbf{r} \frac{n_0(\mathbf{r})}{\tau_T'(\mathbf{r})} = \frac{1}{2\sqrt{2}\,\tau_T^\perp(0)}. \tag{A15}$$

For detailed calculations of various transport relaxation times in a trapped Bose-Einstein-condensed gas, we refer to Ref. [32]. It is straightforward to generalize those calculations to work out the spin transport relaxation times defined above. We find

$$\tau_D^{-1}(\mathbf{r}) = \frac{1}{3} \tau_{\text{cl}}^{-1}(\mathbf{r}), \tag{A16}$$

$$\tau_T^{z-1}(\mathbf{r}) = \frac{3}{5} \tau_{\text{cl}}^{-1}(\mathbf{r}), \tag{A17}$$

$$\tau_T^{\perp-1}(\mathbf{r}) = \frac{7}{15} \tau_{\text{cl}}^{-1}(\mathbf{r}), \tag{A18}$$

where $\tau_{\text{cl}}(\mathbf{r}) \equiv [32n_0(\mathbf{r})a^2(\pi k_BT/m)^{1/2}]^{-1}$ is the mean-collision time. The spatially averaged relaxation rates are given by

$$\gamma_D = \frac{1}{3} \gamma_{\text{cl}}, \quad \gamma_T^z = \frac{3}{5} \gamma_{\text{cl}}, \quad \gamma_T^\perp = \frac{7}{15} \gamma_{\text{cl}}, \quad \delta\gamma_T = -\frac{2}{15} \gamma_{\text{cl}}, \tag{A19}$$

where γ_{cl} is the spatially averaged mean-collision rate

$$\gamma_{\text{cl}} = \frac{16}{\sqrt{2}} n_0(0) a^2 \left(\frac{\pi k_BT}{m}\right)^{1/2}. \tag{A20}$$

In order to compare the moment method directly with our numerical solution of the 1D kinetic equation, we also worked out the three relaxation rates within the simple relaxation time approximation

$$\left.\frac{\partial\vec{\sigma}}{\partial t}\right|_{\text{coll}} = -\frac{\vec{\sigma}(\mathbf{r},\mathbf{p},t) - \vec{M}(\mathbf{r},t)f_0(\mathbf{r},\mathbf{p})}{\tau_{\text{cl}}(\mathbf{r})}. \tag{A21}$$

This simple formula leads to the same collisional contributions in the moment equations as given from the original collision integral, with all the transport relaxation times being replaced with $\tau_{\text{cl}}(\mathbf{r})$, so that one has $\gamma_D = \gamma_T = \gamma_T' = \gamma_{\text{cl}}$. Thus, within the relaxation time approximation, oscillations in the axial and radial directions are completely uncoupled since $\delta\gamma_T = 0$.

[1] N.W. Ashcrof and N.D. Mermin, *Solid State Physics* (Saunders College Publishing, Fort Worth, 1976).

[2] B.R. Johnson, J.S. Denker, N. Bigelow, L.P. Levy, J.H. Freed, and D.M. Lee, Phys. Rev. Lett. **52**, 1508 (1984).

[3] N.P. Bigelow, J.H. Freed, and D.M. Lee, Phys. Rev. Lett. **63**, 1609 (1989).

[4] W.J. Gully and W.J. Mullin, Phys. Rev. Lett. **52**, 1810 (1984).

[5] A.J. Leggett and M.J. Rice, Phys. Rev. Lett. **20**, 586 (1968).

[6] E.P. Bashkin, Pis'ma Zh. Eksp. Teor. Fiz. **33**, 11 (1981) [JETP Lett. **33**, 8 (1981)].

[7] C. Lhuillier and F. Laloe, J. Phys. (France) **43**, 197 (1982).

[8] L.P. Levy and A.E. Ruckenstein, Phys. Rev. Lett. **52**, 1512 (1984).

[9] A.E. Ruckenstein and L.P. Levy, Phys. Rev. B **39**, 183 (1989).

[10] H.J. Lewandowski, D.M. Harber, D.L. Whitaker, and E.A. Cornell, Phys. Rev. Lett. **88**, 070403 (2002).

[11] J.M. McGuirk, H.J. Lewandowski, D.M. Harber, T. Nikuni, J.E. Williams, and E.A. Cornell, Phys. Rev. Lett. **89**, 090402 (2002).

[12] M.O. Oktel and L.S. Levitov, Phys. Rev. Lett. **88**, 230404 (2002).

[13] J.N. Fuchs, D.M. Gangardt, and F. Laloë, Phys. Rev. Lett. **88**, 230404 (2002).

[14] J.E. Williams, T. Nikuni, and C.W. Clark, Phys. Rev. Lett. **88**, 230405 (2002).

[15] A. Kuklov and A.E. Meyerovich, Phys. Rev. A **66**, 023607 (2002).

[16] M.O. Oktel and L.S. Levitov, Phys. Rev. Lett. **83**, 6 (1999).

[17] M.O. Oktel and L.S. Levitov, Phys. Rev. A **65**, 063604 (2002).

[18] T. Nikuni and J.E. Williams (unpublished).

[19] T. Bergeman, G. Erez, and H.J. Metcalf, Phys. Rev. A **35**, 1535 (1987).

[20] D. Guéry-Odelin, F. Zambelli, J. Dalibard, and S. Stringari, Phys. Rev. A **60**, 4851 (1999).

[21] U.A. Khawaja, C.J. Pethick, and H. Smith, J. Low Temp. Phys. **118**, 127 (2000).

[22] D. Guéry-Odelin, Phys. Rev. A **62**, 033607 (2000).

[23] T. Nikuni, Phys. Rev. A **65**, 033611 (2002).

[24] S.D. Gensemer and D.S. Jin, Phys. Rev. Lett. **87**, 173201 (2001).

[25] B. Demarco and D.S. Jin, Phys. Rev. Lett. **88**, 040405 (2002).

[26] H. Smith and H.H. Jensen, *Transport Phenomena* (Clarendon Press, Oxford, 1989).

[27] M.R. Matthews, B.P. Anderson, P.C. Haljan, D.S. Hall, M.J. Holland, J.E. Williams, C.E. Wieman, and E.A. Cornell, Phys. Rev. Lett. **83**, 3358 (1999).

[28] J.E. Williams and M.J. Holland, Nature (London) **401**, 568 (1999).

[29] M.R. Matthews, B.P. Anderson, P.C. Haljan, D.S. Hall, C.E. Wieman, and E.A. Cornell, Phys. Rev. Lett. **83**, 2498 (1999).

[30] E. Zaremba, T. Nikuni, and A. Griffin, J. Low Temp. Phys. **116**, 277 (1999).

[31] B. Jackson and E. Zaremba, Laser Phys. **12**, 93 (2002).

[32] T. Nikuni and A. Griffin, Phys. Rev. A **63**, 033608 (2001); **64**, 049902(E) (2001).

[33] In this paper, the directions "transverse" and "longitudinal" are defined relative to the direction of polarization of the initial spin distribution. Therefore, these terms have a different meaning than in Ref. [14], where the terms are defined relative to the quantization axis of the spin.